IOP Publishing Journal of Physics: Condensed Matter
J. Phys.: Condens. Matter **30** (2018) 264004 (7pp) https://doi.org/10.1088/1361-648X/aac61b

Colloidal transport through trap arrays controlled by active microswimmers

Wen Yang[1], Vyacheslav R Misko[2,3], Fabio Marchesoni[3,4] and Franco Nori[3,5]

[1] College of Materials Science and Engineering, Taiyuan University of Science and Technology, Taiyuan 030024, People's Republic of China
[2] TQC, Universiteit Antwerpen, Universiteitsplein 1, B-2610 Antwerpen, Belgium
[3] Theoretical Quantum Physics Laboratory, RIKEN Cluster for Pioneering Research, Wako-shi, Saitama 351-0198, Japan
[4] Dipartimento di Fisica, Università di Camerino, I-62032 Camerino, Italy
[5] Physics Department, University of Michigan, Ann Arbor, MI 48109-1040, United States of America

E-mail: Vyacheslav.Misko@uantwerpen.be

Received 16 March 2018, revised 13 May 2018
Accepted for publication 18 May 2018
Published 7 June 2018

Abstract

We investigate the dynamics of a binary mixture consisting of active and passive colloidal particles diffusing in a 2D array of truncated harmonic wells, or traps. We explore the possibility of using a small fraction of active particles to manipulate a much larger fraction of passive particles, for instance, to confine them in or extract them from the traps. The results of our study have potential application in biology and medical sciences, for example, to remove dead cells or undesired contaminants from biological systems by means of self-propelled nano-robots.

Keywords: active soft matter, Janus particles, self-propelled motion, binary mixtures, transport, confinement

(Some figures may appear in colour only in the online journal)

1. Introduction

The capture and confinement of passive colloidal particles inside designated areas has been the focus of recent investigations aimed at new protocols for smart drug delivery and targeted cancer therapy [1, 2]. More generally, the study of active self-propelled particles, also called artificial microswimmers, has come to the forefront of biomedical research during the last decade [3–7]. Active particle systems mainly relate to assemblies of either microorganisms, like bacteria [8–12], or artificial self-phoretic colloids, epitomized by the so-called Janus particles [13–17]. Recent advances in the fabrication of active microswimmers suggest new techniques to control diffusion and transport of passive particles in confined geometries. For instance, pumping of passive species by active Janus particles has been demonstrated in asymmetric ratchet channels [18]. Extensive numerical simulations show that in such channels active Janus particles get rectified even in the presence of passive particles and, most remarkably, a tiny fraction of them is capable of dragging along most of the passive species, an effect called 'autonomous pumping' [18]. Recently, persistent dragging of passive colloidal clusters by a single active Janus microswimmer has been observed experimentally even in smooth channels [19].

There have been experimental and theoretical efforts to describe the dynamics of colloidal particles immersed in an active fluid. Most of the reported work addressed the diffusion of colloids in swimming suspensions [20–23] or a passive tracer in a bacteria bath [24–27]. Other studies focused on turbulence in binary mixtures of active and passive particles [28, 29] and the effective interactions between them [30, 31]. While the literature on such binary systems grew drastically in recent years, some basic questions concerning their equilibrium and non-equilibrium statistics remained unanswered.

Recently, the experiments of Koumakis and coworkers [2] demonstrated the targeted delivery of passive colloids by swimming bacteria. These authors designed specific 3D microstructures to serve as targeted area, where bacteria efficiently store the colloidal particles. Inspired by these observations, we simulated a model binary mixture of active Janus

swimmers and passive particles suspended in a confined geometry, like a channel dotted with potential traps. For simplicity, the traps were represented by truncated parabolic potential wells, which closely mimic, for instance, the binding action of actual optical tweezers. We studied the interaction of active and passive species with the purpose of controlling colloidal clustering and transport by means of active microswimmers. In particular, we are interested in devising methods for delivering to and removing passive colloids from a targeted area by fine-tuning the concentration and the self-propulsion parameters of the active microswimmers.

The present paper is organized as follows. Our model and numerical approach are outlined in section 2. The accumulation of particles of mono-species systems within a parabolic trap is reported in section 3.1. Next, in section 3.2 we investigate how effectively the active particles push the passive particles inside the trap. The diffusion of the active particles through trap arrays is simulated in section 3.3. Finally, in section 3.4 we explore the possibility of using active microswimmers to empty the traps from the passive particles stored there. A few concluding remarks are drawn in the final section 4.

2. Model and simulation

In our simulations, N_a active (or self-propelled) particles and N_p passive (or regular colloidal) particles move in a two-dimensional (2D) $L \times L$ box with a parabolic potential well of radius r_D at its center. Periodic boundary conditions are imposed on the box sides. We model both active and passive particles as soft disks of equal radius, r_d, interacting pairwise through a repulsive short-range force. As reported in [18, 32], a particle of coordinates $\mathbf{r}_i = (x_i, y_i)$ is subject to an overdamped dynamics with Langevin equation (LE)

$$\frac{\partial \mathbf{r}_i}{\partial t} = v_0 \hat{\boldsymbol{\nu}}_i + \mu\Big(\sum_{j\neq i} \mathbf{F}_{ij} + \mathbf{F}_i^p\Big) + \boldsymbol{\eta}_i^T(t), \tag{1}$$

where the self-propulsion speed, v_0, is positive only for the active particles, while the mobility, μ, is the same for all constituents of the mixture. Here, $\mathbf{F}_{ij}$ is the repulsive interaction between particles i and j, with $j \neq i$ denoting particles of either species. The particle repulsion force is defined as $\mathbf{F}_{ij} = \kappa\alpha_{ij}\hat{\mathbf{r}}_{ij}$, if $\alpha_{ij} = d - r_{ij} > 0$ and $\mathbf{F}_{ij} = 0$, otherwise. Here, $d = 2r_d$ denotes the particle' diameter, α_{ij} measures the overlap between particles i and j, r_{ij} being the distance between their centers, and, finally, κ is a pair-independent stiffness constant. The attractive force exerted by the trap on particle i is $\mathbf{F}_i^p = -A\mathbf{r}_i$, if $r_i < r_D$ and $\mathbf{F}_i^p = 0$, otherwise. This corresponds to modeling the trap as a truncated harmonic potential well of strength A and radius r_D [33]. The unit vector $\hat{\boldsymbol{\nu}}_i = (\cos\theta_i, \sin\theta_i)$ represents the direction of the self-propulsion velocity of the active particle of index i, the random direction of which, $\theta_i(t)$, is modeled as a Wiener process,

$$\frac{\partial \theta_i}{\partial t} = \eta_i(t), \tag{2}$$

driven by the Gaussian, zero mean-valued, local noise, $\eta_i(t)$, with autocorrelation function

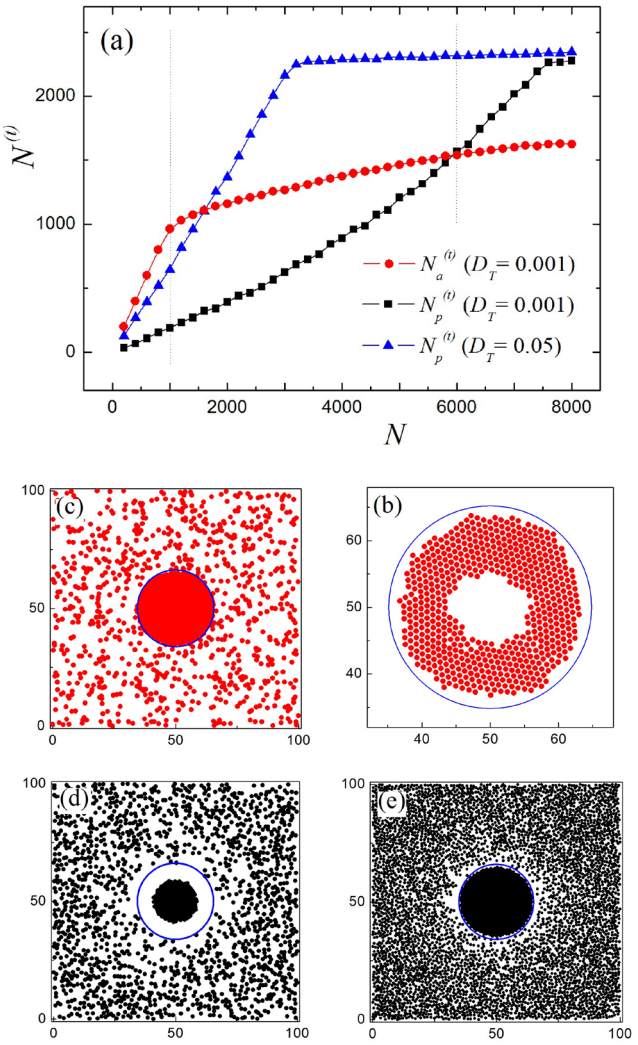

Figure 1. (a) Number of trapped particles, $N^{(t)}$, versus total number of particles, N, for one-species suspensions of passive (squares and triangle) or active particles with $v_0 = 1.0$ (circles). Panels (b)–(e) are snapshots of different systems: (b) $N = N_a = 600$; (c) $N = N_a = 2000$; (d) $N = N_p = 2000$; (e) $N = N_p = 7000$. The circles at the center of the simulation box delimit the parabolic trap. If not specified otherwise, the remaining simulation parameters are $L = 100$, $r_D = 15$, $d = 1$, $A = 0.1$, $\kappa = 10$, $\mu = 1$, $D_r = 0.005$, $D_\mathrm{T} = 0.001$ and $t_e = 6 \cdot 10^4$. The data set represented by triangles in (a) have been obtained for $D_\mathrm{T}^\star = 50D_\mathrm{T}$ and simulation time $t_e^\star = t_e/3$.

$$\langle \eta_i(t)\eta_j(t')\rangle = 2D_r\delta_{ij}\delta(t-t'). \tag{3}$$

Note that the rotational diffusion coefficient, D_r, coincides with the reciprocal of the persistence time, $\tau_r = 1/D_r$, of the exponentially time-correlated Brownian motion executed by a purely active particle [18]. However, here we also consider the effects of thermal fluctuations, represented in equation (1) by the additive Gaussian noise $\boldsymbol{\eta}_i^T(t)$, with correlation functions,

$$\langle \eta_{i\alpha}^T(t)\rangle = 0, \langle \eta_{i\alpha}^T(t)\eta_{j\beta}^T(t')\rangle = 2D_\mathrm{T}\delta_{ij}\delta_{\alpha\beta}\delta(t-t'), \tag{4}$$

where the indices $\alpha = 1, 2$ and $\beta = 1, 2$ denote the Cartesian coordinates x and y, respectively, and D_T is the thermal diffusion coefficient of the suspension.

Furthermore, in order to work with dimensionless quantities, we adopted the particle diameter, d, as the unit of length and the trap relaxation time, $(\mu\kappa)^{-1}$, as the unit of time. Fixed model parameters used in the simulation analysis presented next are $L = 100$, $r_D = 15$, $d = 1$, $A = 0.1$, $\kappa = 10$, $\mu = 1$, $D_r = 0.005$, and $D_{\rm T} = 0.001$. The integration scheme of the model LE's is the same as in [18] with total running time $t_e = 6 \times 10^4$ and integration time-step $\triangle t = 0.001$. In all runs the mixture was initially prepared by generating a uniform random distribution for the positions of the particles and the orientations of the active ones.

In order to emphasize the control action exerted by the active particles on the dynamics of the mixture overall, we kept the levels of the angular, D_r, and thermal noise, $D_{\rm T}$, relatively low. Of course, we ran extensive preliminary numerical tests for a variety of model parameters; the simulation results illustrated below are meant to serve as a proof of concept. For the same reason and to avoid unnecessary complications, we neglected hydrodynamic effects, which are known to contribute to the colloidal pair interaction, especially in 2D [34–36]. Finally, we mention that a similar model, also involving truncated parabolic traps, has already been investigated to study the statistics of a single species of trapped active Janus particles in the long-time ('thermodynamic') limit [33].

3. Simulation results

The system under consideration has two distinct relaxation timescales, one for the active dynamics, τ_a, and one, τ_p, associated with the thermal fluctuations. Both times depend on the trap parameters. The active Brownian motion outside the traps is characterized by the diffusion constant $D_s = v_0^2/2D_r$, which, in our simulation, is much larger than the thermal diffusion $D_{\rm T}$. Accordingly, τ_p turns out to be orders of magnitude larger than τ_a. Under experimental conditions, e.g. in biological systems, τ_a is typically of the order of seconds or minutes, while τ_p can be easily set of the order of hours, days, or even longer. This means that in our discussion τ_p will be regarded as infinitely long. Therefore, we simulated the relaxation dynamics of the binary mixture only up to long-lived quasi-stationary states; that is, states that are stationary on the time scale τ_a. The asymptotic time relaxation toward thermal equilibrium can be numerically investigated only at higher mixture's temperatures, i.e. for values of $D_{\rm T}$ corresponding to numerically accessible (shorter) relaxation times of the trapped passive particles, τ_p.

3.1. Trapping of a single species

In this section we consider suspensions of only active or passive particles in the presence of a trap. In figure 1(a) we plot the number of particles sitting in the trap, $N^{(t)}$ versus the total number of particles of either sort, N, active (red circles) or passive (black squares). We stress that the temperature was taken quite low, such that thermal diffusion is weak, $D_{\rm T} = 0.001$, and the condition $\tau_p \gg \tau_a$ holds. Accordingly, as anticipated above, these results and all system snapshots displayed in panels (b)–(e) of figure 1 have been obtained after simulation times, t_e, obeying the condition $\tau_a < t_e < \tau_p$.

As apparent in figure 1(a), for $N_a < 1000$ all active particles enter the trap, which results in the linear branch of the curve $N_a^{(t)}$ versus N_a with slope equal to one. For $N_a > 1000$, the $N_a^{(t)}$ curve develops a sub-linear behavior which finally levels off for asymptotically large N_a. In contrast, on the same timescale passive particles are uniformly distributed in the box and only a small fraction of them enters the trap. In other words, the spatial diffusion for active particles, figures 1(b) and (c), is much faster than for passive particles, figures 1(d) and (e). The sort of 'halo' surrounding the traps in figures 1(d) and (e) is due to the slow thermal diffusion of the uniformly distributed passive particles, which over the run time length, t_e, fall inside the trap, thus generating a circular depletion region around it.

These distinct relaxation *transient* properties play a crucial role in the dynamics of binary mixtures discussed in the forthcoming sections. In order to access the asymptotic behaviour, i.e. the thermodynamic equilibrium limit, one should considerably increase either the simulation time or the temperature. In figure 1(a) we plot, as an example, the curve $N_p^{(t)}$ versus N_p for a much larger thermal diffusion, $D_{\rm T}^\star = 50 D_{\rm T}$, but using a shorter simulation time, $t_e^\star = t_e/3$. Under such conditions, the passive particle suspension behaves similarly to the active suspension described above, namely, exhibits a linear growing branch corresponding to the trapping of all passive particles for $N_p < 3000$ and an asymptotic saturation for much larger N_p. However, as an interesting difference, one notices that here the horizontal asymptote is relatively higher and sets in immediately around $N_p = 3000$, that is after the trap has been filled up. This is an obvious effect of the self-propulsion mechanism, which eventually hinders the containment of the active particles inside the trap.

3.2. Trapping of passive particles assisted by Janus microswimmers

We inject now an increasing number of Janus particles, N_a, into a suspension containing a fixed number of passive particles, $N_p = 1000$. In figure 2(a) we plot the number of trapped passive particles, $N_p^{(t)}$, versus N_a, for increasing values of the self-propulsion speed of the active microswimmers. The number of Janus particles trapped at the same time, $N^{(t)}$, is displayed in figure 2(b) for comparison.

A few properties of the mixture transient dynamics are apparent. First of all, trapping of passive particles is clearly expedited by the presence of active particles and grows more efficient upon increasing the concentration of the active component in the mixture.

More interesting is the dependence of the curves $N_p^{(t)}$ versus N_a of figure 2(a) on the speed of the active Janus swimmers, v_0. $N_p^{(t)}$ first grows linearly (and slowly) with N_a up to certain critical value, $N_a^\star$, and then bends upward toward its saturation value, $N_p \simeq 1000$. Such a sudden jump in the curves' profile shifts towards lower N_a with increasing v_0, until the linear branch disappears altogether for $v_0 > 1.5$. All

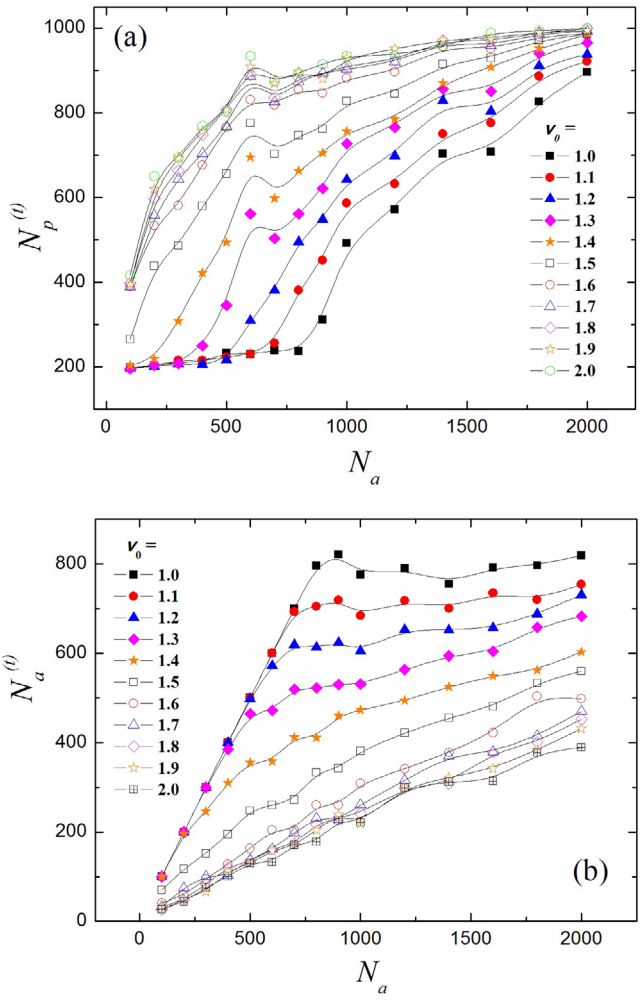

Figure 2. (a) Number of trapped passive particles in the trap $N_p^{(t)}$ versus total active particle number, N_a, for $N_p = 1000$ and different v_0 (see legend). (b) The corresponding number of active particles, $N_a^{(t)}$, trapped at the same time. Note that the simulation data are represented by symbols, while the smooth interpolating curves are just a guide to the eyes. If not indicated otherwise, all simulation parameters are as in figure 1.

curves in figure 2(a) exhibit a small bump at about $N_a = 600$, which gets more prominent as $N_a^\star$ approaches zero. The origin of these bumps is related with the formation of shells of active particles inside the trap (see snapshots in figure 3 for $N_a = 500$ and 600). For $N_a \leqslant 600$, the filling of the trap with active particles is proportional to N_a (with slope close to 1 for v_0 up to 1.3, see figure 2(b)). Such 'quasi-stationary' shells encage passive particles inside the trap. The number of active particles in the shells saturates at about $N_a^{(t)} \approx 600$, as shown by the curves of figure 2(b) for $v_0 = 1.3$–1.5. The observed bumps in figure 2(a) correspond to these plateaus. Their appearance means that additional active particles do not contribute to the active shells surrounding the passive particles in the trap. These additional active particles thus freely move in and out of the trap, which eases the escape of the passive particles.

Moreover, one notices that for $v_0 = 2.0$ and $N_a \approx 600$ about 95% of the passive particles become trapped, whereas

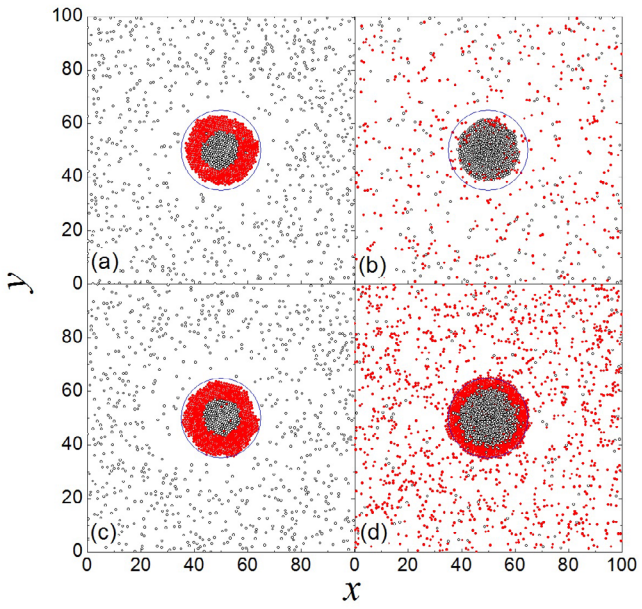

Figure 3. (a)–(d) Snapshots of the spatial configuration of a mixture with $N_p = 1000$ (a) $N_a = 500$, $v_0 = 1.0$; (b) $N_a = 500$, $v_0 = 2.0$; (c) $N_a = 600$, $v_0 = 1.0$; and (d) $N_a = 2000$, $v_0 = 1.0$. All remaining simulation parameters are as in figure 1. The circles at the center of the simulation box delimit the parabolic trap.

in the absence of active swimmers only slightly more than 20% of them are found in the trap. This validates our starting idea of using active swimmers to control the dynamics of passive colloids: active swimmers do efficiently help trap passive particles; they can be employed to clear up a working area from undesired stray particles by storing them in targeted areas, represented here by traps.

Simultaneously, as illustrated in figure 2(b), the number of dynamically trapped active particles, $N_a^{(t)}$, also increases with their total number, N_a. However, the dependence of the curves $N_a^{(t)}$ versus N_a on v_0 is opposite to that observed for the passive mixture fraction: At a fixed concentration of Janus microswimmers, $N_a^{(t)}$ markedly decreases with increasing v_0. Therefore, the simulation data of figure 2(b) indicate that for the system parameters yielding the maximum trapping of the passive particles, i.e. $N_a = 600$ and $v_0 = 2.0$, only about 15% to the active swimmers sit inside the trap.

The findings of figures 1 and 2 can be summarized as follows. A small fraction of active swimmers of relatively high self-propulsion speed ('hot' swimmers) added to a suspension of passive particles can drastically change the diffusive dynamics of the mixture overall. In particular, they can be used to confine the passive particles inside a designated storing area with efficiency that can be thus enhanced by a factor of up to four, or even larger.

Examples of the spatial distribution of active (red) and passive (black) particles in the simulation box at low temperature, $D_T = 0.001$, are presented in figure 3. The snapshots of panels (a) and (c) illustrate situations when the trap apparently contains all active particles and only a small fraction of the passive ones. This occurrence is typical for low self-propulsion speeds; here, $v_0 = 1.0$. 'Heating up' the system by raising

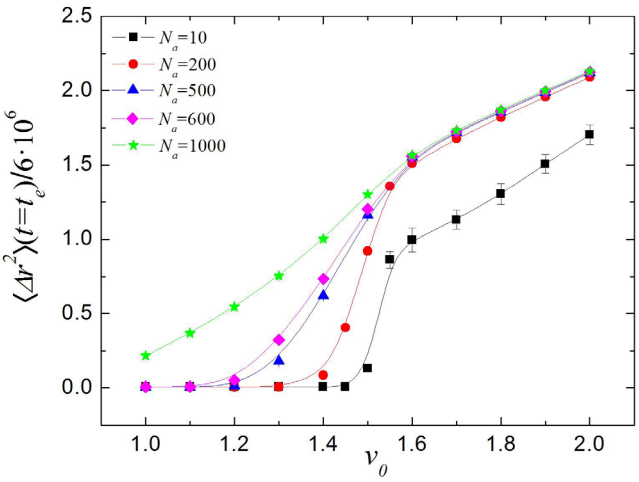

Figure 4. Mean square displacement, $\langle \Delta r^2 \rangle$ for $t = t_e$, of active particles as a function of v_0, for systems with $N_p = 1000$ and varying N_a (see legends). Error bars are larger than the symbols only for $N_a = 10$ and $v_0 > 1.5$. Interpolating curves are a guide to the eye. All remaining simulation parameters are as in figure 1.

v_0 from 1.0 up to 2.0 sharply changes the quasi-stationary mixture configuration: The initially 'sleeping' active Janus swimmers leave the trap and 'heat up' the passive component of the suspension. Under the stirring action of the Janus microswimmers, the passive particles then edge toward and eventually fall inside the trap in larger numbers, as shown in figure 3(b). On the contrary, the microswimmers themselves, due to their high motility, can easily escape from the trap. A simple force-balance argument yields the depinning condition $v_0 > \mathrm{Ar}_D$, i.e. $v_0 > 1.5$ for the simulation parameters of figure 3. Of course, active particles can populate the area outside the trap also for lower self-propulsion speeds, but only at much higher concentrations, like in figure 3(d).

We recall that the above mechanism is a transient effect that works only for $\tau_a \ll \tau_p$. In our simulations such condition was ensured by taking a very small thermal diffusion, $D_\mathrm{T} = 0.001$, and a long simulation time, $t_e = 6 \cdot 10^4$, so that $L^2 \gg 4 D_\mathrm{T} t_e$. At high temperatures, when the spatial diffusion induced by thermal fluctuations becomes appreciable, see figure 1(a), the above condition breaks down and the dynamical behaviour of active and passive species becomes indistinguishable (not shown). The latter occurrence represents an equilibrium condition clearly expected in the asymptotic time limit, but of lesser usage for practical applications.

3.3. Mean square displacement

The diffusive properties of the mixture constituents are characterized by their mean square displacement (MSD) defined as $\langle \Delta r^2(t) \rangle = \langle [r(t) - r(0)]^2(t) \rangle$. To analyze the diffusion of the active fraction, in figure 4 we plotted the MSD of the active Janus particles taken at $t = t_e$, $\langle \Delta r^2(t = t_e) \rangle \equiv \langle \Delta r^2(v_0) \rangle$, versus v_0 for different concentrations, N_a, and a fixed number of passive particles, $N_p = 1000$. The ensemble average (respectively over $N_a = 10$,200,500,600 and 1000 active particles) was further averaged over five independent simulation runs to obtain the rather smooth curves displayed in figure 4.

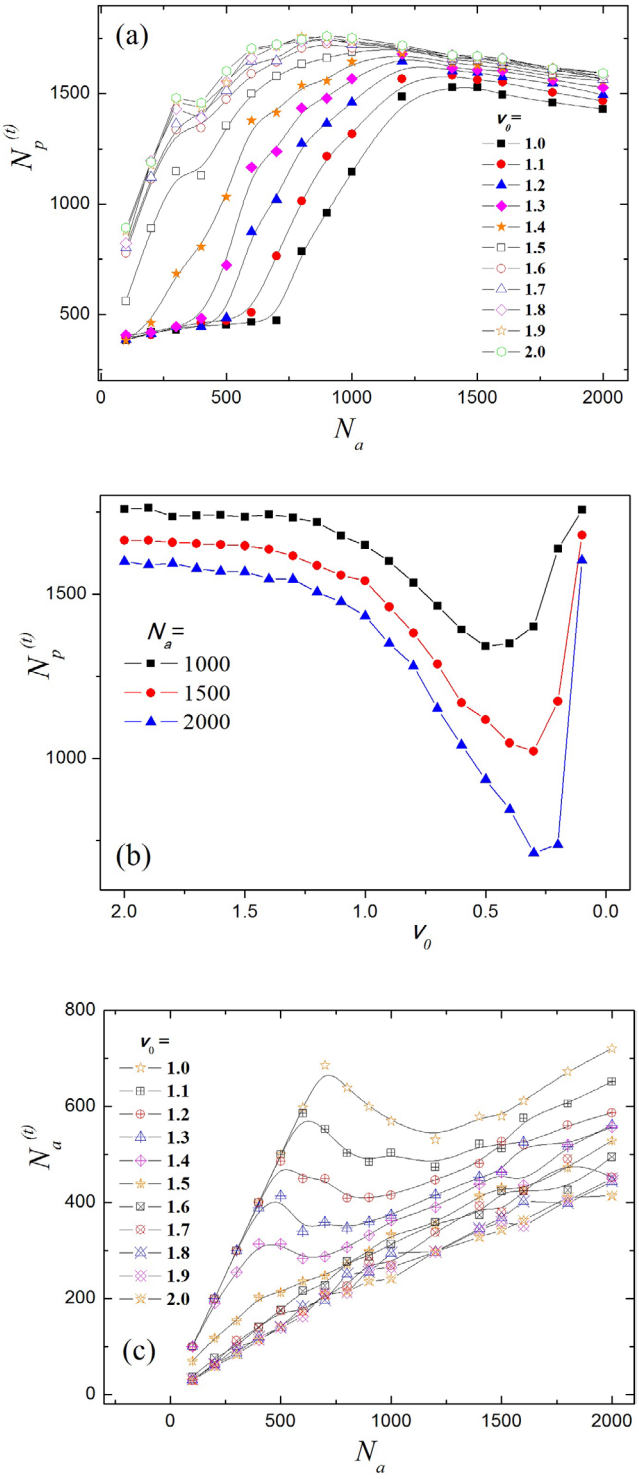

Figure 5. (a) Number of passive particles in the trap, $N_p^{(t)}$ versus total active particle number, N_a, for $N_p = 2000$ and different v_0 (see legend). (b) Detrapping of passive particles (initially all placed in the trap): $N_p^{(t)}$ versus v_0 for $N_p = 2000$ and different N_a (see legend). (c) The number of active swimmers in the trap corresponding to (a). All the remaining simulation parameters are as in figure 1. Interpolating curves are a guide to the eye.

For relatively low concentrations, $N_a < 600$, active Janus microswimmers with $v_0 < \mathrm{Ar}_D$ are strongly confined by the trap, so that for $v_0 = 1.0$–1.2 we obtained $\langle \Delta r^2 \rangle \simeq 0$.

Increasing the self-propulsion speed across the range 1.4–1.6 causes a quite abrupt MSD jump, which we relate to the escape, or depinning of the Janus particles from the trap. Finally, for even higher self-propulsion speeds, $v_0 = 1.6$–2.0, the MSD appears to linearly increase with v_0. We explain this effect by invoking the high rate of collisions between active and passive particles occurring outside the trap. In contrast to the above picture, at high active swimmer concentrations, e.g. $N_a = 1000$, the MSD depinning jump tends to disappear. In this regime, the almost linear dependence of the MSD on v_0 is related to the observation that, due to their large concentration, the number of microswimmers diffusing outside the trap is appreciable even at low v_0 and surely increases with it. Vice versa, the depinning step of the MSD curves becomes sharper and sharper as N_a is lowered. Note that in figure 4 the step for $N_a = 10$ occurs at $v_0 = 1.5$, as predicted.

3.4. Detrapping of passive particles assisted by Janus microswimmers

In section 3.2 we showed how active Janus particles can help store a large amount of passive particles in the trap. That result was achieved by injecting a small fraction of strongly self-propelled (or 'hot') Janus swimmers in the passive suspension. This technique, in turn, raises a naturally related question that is especially meaningful in view of future applications: How can we remove the passive particles from the trap after they have accumulated there?

One simple method is suggested by inspecting the snapshots of the mixture configuration shown in figures 3(a) and (c): one can 'cool down' the active component of the mixture, that is slow down the active Janus swimmers. To analyze this process in detail, we first calculated the number of trapped passive particles, $N_p^{(t)}$, versus the number of active particles, N_a, assuming that the former were initially distributed *at random* in space. The results are shown in figure 5(a) for different values of v_0. In contrast, to model detrapping all passive particles were initially placed *inside* the trap. As discussed at the top of section 3, the number of trapped passive particles, $N_p^{(t)}$, clearly depends on the initial conditions. Indeed, the detrapping rate of initially trapped passive particles will be lower than of randomly distributed passive particles. This hysteretic behavior is due to the fact that the simulation time, t_e, is much larger (shorter) than the relaxation time of the active (passive) particles. Therefore, all observables, like $N_p^{(t)}$, calculated over the run time t_e are independent of the initial configurations of the active particles, but do depend, in general, on the initial distribution of the passive particles. Therefore, we chose three initial values of $N_p^{(t)}$ (resulting from the preparation procedure of figure 5(a), respectively, for $N_a = 1000$, 1500 and 2000) and then simulated the two species mixture by *decreasing* v_0 stepwise from the initial value 2.0 down to 0.1. Finally, figure 5(c) shows the number of trapped active swimmers corresponding to the situation shown in panel (a).

One notices immediately that $N_p^{(t)}$ in 5(a) exhibits a nonmonotonic dependence on N_a, which is consistent with the numerical data of figure 2(a). More remarkably, however, in figure 5(b) $N_p^{(t)}$ decreases monotonically with lowering v_0 from 2.0 down to around 0.5. A minimum trap occupancy is achieved for values of v_0 that grow lower as N_a is raised. Therefore, by 'cooling down' the active mixture component, we can actually extract a substantial fraction of passive particles stored in the trap.

4. Conclusions

We have investigated the diffusive dynamics of a binary suspension of active Janus swimmers and passive colloidal particles in the presence of a local confining potential (trap). We have demonstrated the possibility of spatially manipulating the passive particles by means of the active swimmers with particular attention to their storing in and extraction from the trap. The former task was performed by injecting in the system a small fraction of active Janus swimmers with high self-propulsion speed ('hot' swimmers). The latter task, instead, was achieved by 'cooling down' the active component of the mixture. In real experiments the speed of the self-propelled motion can be easily controlled, for instance, by regulating the intensity of the light illuminating the Janus microswimmers (thermo-phoresis) or the fuel concentration in the solution (chemo-phoresis).

Acknowledgments

This work was supported by the FWO-JSPS bilateral project, the 'Odysseus' Program of the Flemish Government and the Flemish Research Foundation (FWO-Vl) (Belgium). WY acknowledges the support from NSFC (No. 11204199), Shanxi Scholarship Council (No. 2016-096), Fund for Shanxi Key Subjects Construction of China. FN is partially supported by the MURI Center for Dynamic Magneto-Optics via the AFOSR Award No. FA9550-14-1-0040, the Army Research Office (ARO) under grant number 73315PH, the AOARD grant No. FA2386-18-1-4045, the IMPACT program of JST, JSPS-RFBR Grant No. 17-52-50023, CREST Grant No. JPMJCR1676, the RIKEN-AIST Challenge Research Fund, and the Sir John Templeton Foundation.

ORCID iDs

VyacheslavRMisko https://orcid.org/0000-0002-5290-412X
Fabio Marchesoni https://orcid.org/0000-0001-9240-6793
Franco Nori https://orcid.org/0000-0003-3682-7432

References

[1] Palacci J, Sacanna S, Vatchinsky A, Chaikin P M and Pine D J 2013 *J. Am. Chem. Soc.* **135** 15978
[2] Koumakis N, Lepore A, Maggi C and Di Leonardo R 2013 *Nat. Commun.* **4** 2588
[3] Dreyfus R, Baudry J, Roper M L, Fermigier M, Stone H A and Bibette J 2005 *Nature* **437** 862
[4] Ozin G A, Manners I, Fournier-Bidoz S and Arsenault A 2005 *Adv. Mater.* **17** 3011

[5] Palacci J, Sacanna S, Steinberg A P, Pine D J and Chaikin P M 2013 *Science* **339** 936
[6] Buttinoni I, Bialke J, Kummel F, Lowen H, Bechinger C and Speck T 2013 *Phys. Rev. Lett.* **110** 238301
[7] Yang W, Misko V R, Nelissen K, Kong M and Peeters F M 2012 *Soft Matter* **8** 5175
[8] Petroff A P, Wu X-L and Libchaber A 2015 *Phys. Rev. Lett.* **114** 158102
[9] Dunkel J, Heidenreich S, Drescher K, Wensink H H, Bar M and Goldstein R E 2013 *Phys. Rev. Lett.* **110** 228102
[10] Lauga E and Goldstein R E 2012 *Phys. Today* **65** 30
[11] Drescher K, Leptos K C, Tuval I, Ishikawa T, Pedley T J and Goldstein R E 2009 *Phys. Rev. Lett.* **102** 168101
[12] Darnton N C, Turner L, Rojevsky S and Berg H C 2007 *J. Bacteriol.* **189** 1756
[13] Yan J, Bloom M, Bae S C, Luijten E and Granick S 2012 *Nature* **491** 578
[14] Zhao Y, Shum H C, Chen H, Adams L L A, Gu Z and Weitz D A 2011 *J. Am. Chem. Soc.* **133** 8790
[15] Jiang H-R, Yoshinaga N and Sano M 2010 *Phys. Rev. Lett.* **105** 268302
[16] Jiang S, Chen Q, Tripathy M, Luijten E, Schweizer K S and Granick S 2010 *Adv. Mater* **22** 1060
[17] Tang C, Zhang C, Liu J, Qu X, Li J and Yang Z 2010 *Macromolecules* **43** 5114
[18] Ghosh P K, Misko V R, Marchesoni F and Nori F 2013 *Phys. Rev. Lett.* **110** 268301
[19] Yu H L, Kopach A, Misko V R, Vasylenko A A, Makarov D, Marchesoni F, Nori F, Baraban L and Cuniberti G 2016 *Small* **12** 5882
[20] Molina J J and Yamamoto R 2014 *Mol. Phys.* **112** 1389
[21] Valeriani C, Li M, Novosel J, Arlt J and Marenduzzo D 2011 *Soft Matter* **7** 5228
[22] Gregoire G, Chate H and Tu Y 2001 *Phys. Rev.* E **64** 011902
[23] Wu X and Libchaber A 2000 *Phys. Rev. Lett.* **84** 3017–20
[24] Morozov A and Marenduzzo D 2014 *Soft Matter* **10** 2748
[25] Kasyap T V, Koch D L and Wu M 2014 *Phys. Fluids* **26** 081901
[26] Mallory S A, Valeriani C and Cacciuto A 2014 *Phys. Rev.* E **90** 032309
[27] Kaiser A and Lowen H 2014 *J. Chem. Phys.* **141** 044903
[28] Su Y-S, Wang H-C and Lin I 2015 *Phys. Rev.* E **91** 030302
[29] Liu K-A and Lin I 2013 *Phys. Rev.* E **88** 033004
[30] Angelani L, Maggi C, Bernardini M L, Rizzo A and Di Leonardo R 2011 *Phys. Rev. Lett.* **107** 138302
[31] Krafnick R C and Garcia A E 2015 *Phys. Rev.* E **91** 022308
[32] Fily Y and Marchetti M C 2012 *Phys. Rev. Lett.* **108** 235702
[33] Yang W, Misko V R, Tempere J, Kong M H and Peeters F M 2017 *Phys. Rev.* E **95** 062602
[34] Di Leonardo R, Keen S, Ianni F, Leach J, Padgett M J and Ruocco G 2008 *Phys. Rev.* E **78** 031406
[35] Yang X, Liu C, Li Y, Marchesoni F, Hänggi P and Zhang H P 2017 *Proc. Natl Acad. Sci. USA* **114** 9565
[36] Debnath T, Li Y, Ghosh P K and Marchesoni F 2018 *Phys. Rev.* E **97** 042602